Structure of the Subgel (Lc') and Gel (L.beta.') Phases of Oriented Dipalmitoylphosphatidylcholine Multibilayers

ARTICLE *in* THE JOURNAL OF PHYSICAL CHEMISTRY · MARCH 1995

Impact Factor: 2.78 · DOI: 10.1021/j100012a039

1 AUTHOR:

John Katsaras
Oak Ridge National Laboratory
240 PUBLICATIONS **4,724** CITATIONS

SEE PROFILE

Reprinted from The Journal of Physical Chemistry, 1995, 99.

Structure of the Subgel ($L_{c'}$) and Gel ($L_{\beta'}$) Phases of Oriented Dipalmitoylphosphatidylcholine Multibilayers

J. Katsaras

Centre de Recherche Paul Pascal-CNRS, Avenue Albert Schweitzer, F-33600 Pessac, France, and AECL Research, Neutron and Condensed Matter Science, Chalk River Laboratories, Chalk River, Ontario, K0J 1J0 Canada

Received: June 24, 1994; In Final Form: October 10, 1994[⊗]

An X-ray study of highly oriented films of 1,2-dipalmitoyl-*sn*-glycero-3-phosphatidylcholine (DPPC) in the $L_{c'}$ phase is presented. The data describe the physical characteristics of the hydrophilic phosphorylcholine headgroups and hydrocarbon chains in the $L_{c'}$ phase and show that the $L_{c'} \rightarrow L_{\beta F}$ phase transition is characterized by a change in hydrocarbon chain packing, tilt angle and direction. Also, 1D electron density profiles indicate that $L_{c'}$ and dry $L_{\beta F}$ bilayers differ significantly in the bilayer interface region from those in the $L_{\beta I}$ (molecular tilt toward nearest neighbors) and hydrated $L_{\beta F}$ (molecular tilt between nearest neighbors) phases.

Introduction

In 1980 Chen et al.[2] observed a third phase transition centered at about 18 °C in a DPPC multilamellar suspension using differential scanning calorimetry (DSC). Until then, DPPC suspensions were known to have only two thermotropic phase transitions. The main gel-to-liquid crystalline phase transition ($T_m \approx 41$ °C) and a broader so-called "pretransition" ($T_m \approx 35$ °C). However this newly discovered phase was observed only after Chen and co-workers[2] stored the multilamellar suspension of DPPC at ≈0 °C for several days. Since then, there have been many experiments carried out to characterize the structure of the subgel phase.[3-11]

In excess water preparations,[12] it is generally known that $L_{\beta'}$ DPPC multilamellar vesicles have a lamellar periodicity (d) of ≈64 Å and characteristic wide-angle reflections at 1/4.2 $Å^{-1}$ (020) and 1/4.1 $Å^{-1}$ (110).[4,5,13] However upon storage for several days at 0 °C, a structural transformation occurs whereby d decreases to ≈59 Å and the wide-angle reflections have values of 1/4.4 $Å^{-1}$ (020) and 1/3.9 $Å^{-1}$ (110).[3-5] In addition, reflections due to the ordering of the DPPC molecules in the plane of the bilayer are also observed.[11] This latter phase is known as either the L_c or $L_{c'}$ phase, and it is generally accepted that in maximally hydrated DPPC samples the $L_{\beta I} \rightarrow L_{c'}$ transition involves dehydration and hydrocarbon chain reorganization.[4-6]

In this paper we report a detailed structural investigation, using X-ray diffraction, of the subgel $L_{c'}$ and gel $L_{\beta'}$[14] phases of highly oriented samples of DPPC. We show that the $L_{c'}$ samples, at ≈65% relative humidity, undergo a phase transition into the $L_{\beta F}$ phase and experience the following changes: (a) Hydrocarbon chain lattice symmetry changes from oblique to rectangular. (b) The chain tilt angle θ with respect to the bilayer normal is reduced. (c) Change in the lattice tilt direction from fatty acid chains being tilted approximately toward nearest neighbor to being tilted between nearest neighbor. On the other hand, ≈85% RH $L_{c'}$ bilayers undergo a transition into the $L_{\beta I}$ phase. In addition, 1D electron density profiles indicate that $L_{c'}$ and dry $L_{\beta'}$ bilayers differ significantly in the bilayer interface region from those in the $L_{\beta'}$ phase which have been hydrated. This difference is probably due to the absence of rapid transitions of the diacylglycerol group between different minimum free energy states in the $L_{c'}$ and dry $L_{\beta'}$ phases. Finally, the chain tilt angle θ is greater in $L_{c'}$ bilayers compared to those in the $L_{\beta I}$ phase as a result of the hydrocarbon chains in the $L_{c'}$ phase having a smaller cross-sectional area (≈3%).

Experimental Section

1,2-Dipalmitoyl-*sn*-glycero-3-phosphatidylcholine (DPPC) was obtained from Avanti Polar Lipids Inc. (Birmingham, AL) and oriented on the surface of a 30-mL Pyrex beaker (No. 1000) using a concentrated solution of DPPC and methanol which was pipetted onto the surface of the beaker. After evaporation of the methanol, a clear film of lipid was left adhering to the outside of the beaker. The remainder of the methanol was removed by placing the samples under a vacuum for 24 h, after which time they were hydrated in ≈100% relative humidity (RH) environment for a few days. 0% RH samples were obtained by placing hydrated samples under a vacuum for 48 h. To obtain oriented $L_{c'}$ DPPC bilayers, samples were placed at 4 °C for 5 days. The preparation of oriented bilayers on a curved glass surface from a concentrated solution of methanol produces a stack of ≈2000 highly oriented (<5° mosaic spread) bilayers.

The experiments were caried out with an 18-kW Rigaku Rotaflex RU300 rotating anode generator and a 2D Marresearch imaging plate detector having a plate diameter of 180 mm and a pixel size of 150 μm × 150 μm. Monochromation of the Cu radiation was achieved using a flat graphite crystal having a mosaic spread of 0.4 ± 0.1° $\text{fwhm}_{(002)}$ and the sample-to-film distance was 185 ± 1 mm. The spot size, as defined by three sets of vertical and horizontal slits, was approximately 0.5 mm × 0.5 mm. As a result of the 2D detector and curved sample holder (X-ray beam passed through the sample tangent to the vertical curved side of the beaker), we were able to obtain simultaneously both in-plane structure (wide-angle reflections) and the layer spacing (small-angle reflections, c^*).

The sample holder (volume ≈ 300 cm^3) was designed to monitor and control both the RH and the temperature. For samples at 20 °C, the RH was adjusted by varying the flow rate of N_2 or N_2 through water in a gas washer before passage through the sample holder. For samples at a relatively constant humidity and various temperatures, the RH was adjusted by either pure water (85 ± 10% RH) or an NaCl–water solution (65 ± 10% RH). The RH was monitored by a digital hygrometer (Vaisala HMI 31; Helsinki, Finland) and the

[⊗] Abstract published in *Advance ACS Abstracts,* February 15, 1995.

0022-3654/95/2099-4141$09.00/0

temperature controlled by a Haake water bath (Berlin, Germany). Our lower than expected values for the RH were due to the presence of temperature gradients in our sample holder at temperatures less than ambient.

Reconstruction of the Electron Density Profiles. An experimental limitation lies in the fact that from a diffraction pattern the intensities are recorded without information about phase. However, in lipid bilayers and other lyotropic centrosymmetric systems, it is possible to assign phases by swelling the structure and mapping out the changes in intensity for the various Bragg reflections.[15-17] The phases of the various reflections were determined by this method and reconstructing the continuous transforms using the communication theory by Shannon.[18,19] The continuous transform, F_R, is simply constructed by laying down the function $F_h[(\sin \pi\ dx)/\pi\ dx]$ at points $x = h/d$ ($h = 0, 1, 2, ..., n$) with the amplitude of the function (F_h) being equal to the amplitude of the structure factor at that point and adding. The sign of the amplitude is determined by the phase. The amplitude of the structure factor is the square root of the corrected intensity. Finally, the intensities, I_h, were obtained by integrating the Bragg reflections (along the c^* axis), due to the stacked bilayers, after background subtraction and corrected using a half-Lorentz correction; that is, the intensities were multiplied by the order of the diffraction peak, h.[20]

For various RHs, the correct phase assignments result in a family of transforms which give an appearance of simplicity and uniqueness in the case where the motif (lipid bilayer) has changed in a simple way during swelling (e.g., changes in the hydrocarbon chain tilt angle with increasing hydration).[16,17] In the case where there is no change to the motif as a function of humidity, the calculated continuous transforms should lie on top of each other.[17] The zeroth-order amplitude, necessary for the reconstruction of the continuous transforms but whose accuracy is not crucial, was calculated by subtracting the electron density of water from the average electron density of the bilayer and multiplying by the repeat spacing.[21]

Experimental Results and Analysis

In Figure 1 we present an electron density profile containing 1.5 bilayer units constructed to a resolution of ≈4 Å and a corresponding model of a lipid bilayer having its hydrocarbon chains tilted at an angle θ with respect to the bilayer normal. The interpretation of 1D electron density profiles is by now well understood.[16] The low electron density trough is attributed to the terminal methyl groups while the maxima correspond to the phosphate moieties of the polar phosphorylcholine headgroups (highest electron density) and the ester groups of the hydrocarbon chains. The methylene groups of the hydrocarbon chains are depicted in the 1D profile as regions of relative uniform electron density while the region between the two most electron dense peaks is generally known as the "water region". The thickness of the water layer region gives some indication of the relative amounts of water present in the sample.

Figure 2 shows diffraction patterns of $L_{c'}$ bilayers (Figure 2a) at 17 °C having a repeat spacing (d) of 56.3 Å (≈65% RH) and 58.7 Å $L_{\beta F}$ bilayers (Figure 2b) at 20 °C along with their 1D electron density profiles (insets). It is important to note that diffraction patterns from $L_{c'}$ bilayers at 5 and 10 °C (not shown) were similar to the diffraction pattern presented in Figure 2a. In both the $L_{c'}$ and $L_{\beta F}$ phases, the diffraction maxima at wide angles are in the form of short bars (parallel to c^*) whose lengths are $>c^*$ (distance between two successive Bragg peaks) giving an out-of-plane correlation length of <1 bilayer.[14]

In bilayer systems where the hydrocarbon chains of the lipid are not tilted, one would expect two wide-angle maxima

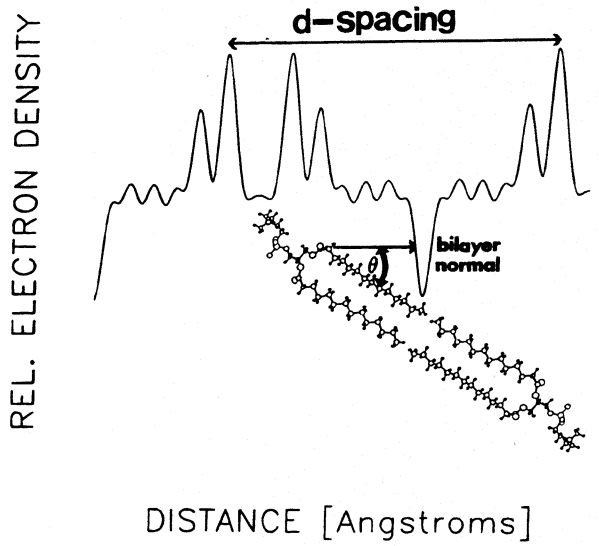

Figure 1. 1D electron density profile showing 1.5 bilayer units constructed to a resolution of ≈4 Å and a corresponding lipid bilayer whose hydrocarbon chains are tilted at an angle θ with respect to the bilayer normal. The relatively flat portion of the profile corresponds to the CH_2 groups of the hydrocarbon chains while the low electron density troughs are due to the terminal CH_3 groups. The region between the peaks due to the phosphate moiety of the polar phosphorylcholine headgroup is generally known as the "water region" and changes with changes in hydration.

centered on the equatorial axis (perpendicular to the c^* axis). However, both the $L_{c'}$ and $L_{\beta F}$ phases presented in Figure 2 exhibit off-equatorial reflections indicating that the hydrocarbon chains of the lipid molecules in these phases are tilted with respect to the bilayer normal.[14] In the $L_{c'}$ phase, the (020) reflection has a maximum centered at ≈5° off of the equator while the off-equatorial (110) (≈1/3.9 $Å^{-1}$) and ($1\bar{1}0$) (≈1/3.8 $Å^{-1}$) reflections are unique, indicating that the unit cell is oblique.[22] In this case we have chosen an oblique centered unit cell for continuity with the centered rectangular unit cell found in all of the $L_{\beta'}$ phases. From the above wide-angle information we can say that the hydrocarbon chains are tilted at an angle θ of 34.2 ± 1.0° toward a nearest neighbor in the (020) plane (please see Appendix).

Figure 3a contains the continuous Fourier transforms, reconstructed by use of the communication theorem, for DPPC bilayers in the $L_{c'}$ phase.[18] The 1D electron density profile in Figure 2a (inset) was obtained through the phase assignment procedure mentioned in a previous section, and which makes no assumptions about the structure of the system. The only model-based calculation has to do with a rough approximation of the zeroth-order amplitude. However, in the larger value reciprocal space regions (>0.1 $Å^{-1}$), where phase uncertainties exist, the transform is practically free from the influence of the zeroth order and as such, so is the model.[16] In Figure 3a we present a family of transforms, corresponding to $L_{c'}$ bilayers, which expand uniformly in reciprocal space as a function of hydration. This implies that with increasing hydration there is a decrease in the thickness of the bilayer (the motif) as a result of small changes to the tilt angles of the various $L_{c'}$ bilayers. This result is in agreement with the hydrocarbon chain tilt angles which one can measure from the X-ray diffraction patterns (please see Figures 2a and 6a). Attempting to change the phase of a single reflection (e.g., ninth order + instead of −) results in a "complicated" family of transforms which do not exhibit any systematic change with hydration (Figure 3b). The 1D electron density profile of 65% RH bilayers having a ninth-order phase of + instead of − (Figure 2a inset) is given in Figure

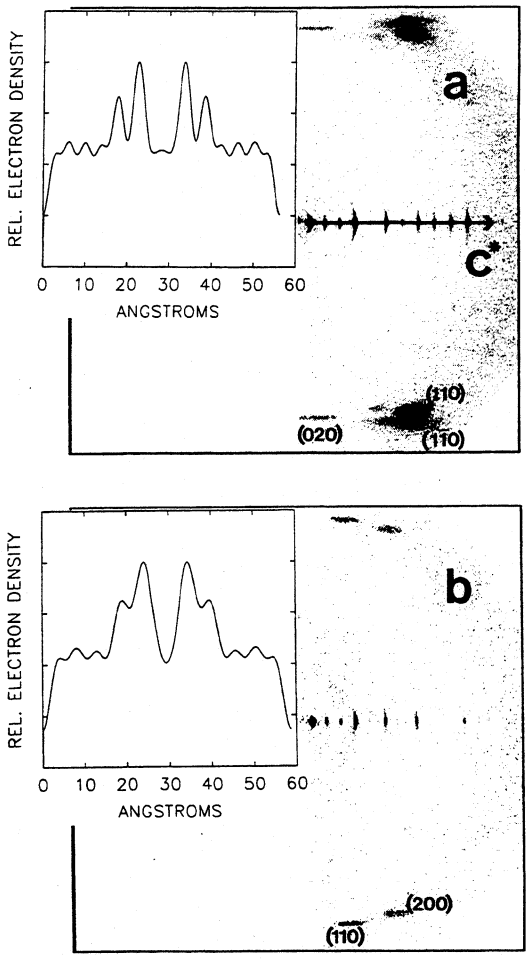

Figure 2. 2D diffraction patterns and 1D electron density distributions (insets) of (a) 65% RH $L_{c'}$ DPPC bilayers having a d spacing of 56.3 Å at 17 ± 2 °C; (b) 58.7 Å $L_{\beta F}$ bilayers at 20 ± 2 °C. The calculated tilt angles θ are 34.2 ± 1.0° and 26.3 ± 0.5° for the $L_{c'}$ and $L_{\beta F}$ phases, respectively. In the $L_{c'}$ phase, the splitting angles measured from the diffraction patterns due to the (020), (1$\bar{1}$0), and (110) reflections are 5.0, 28.8, and 31.9°, respectively. The (020), (1$\bar{1}$0), and (110) reflections of the $L_{c'}$ phase have $1/d$ spacings of 1/4.4, 1/3.9, and 1/3.8 Å^{-1}, respectively. For the $L_{\beta F}$ phase, the splitting angles for the (110) and (200) reflections are 14.1 and 26.3°, respectively. The (110) and (200) reflections both have $1/d$ spacings of 1/4.1 Å^{-1}. The splitting angle measurements contain an error of ±0.5° while the d spacings have errors of ±0.3 Å.

3c. Comparison of Figures 2a (inset) and 3c shows that the biggest difference between the two electron density distributions lies in the hydrocarbon chain region.

Although the procedure described for assigning phases by Torbet and Wilkins[16] makes no assumptions about the bilayer's structure, we feel that the use of such assumptions to test the correctness of the phases and as such, the structure, are justified. As mentioned previously, the most noticeable difference between Figures 2a (inset) and 3c is to be found in the hydrocarbon chain region (0−15 Å). Since the hydrocarbon chain region in DPPC molecules consists of 14 CH_2 groups, one would expect the electron density profile of a bilayer to be rather uniform in this region. Of the two electron density functions, the one that approaches the "expected" profile corresponds to the structure whose phases were chosen by the swelling procedure.

Going to the $L_{\beta F}$ phase (Figure 2b), one can observe that there are no reflections centered on the equatorial axis, implying that there is a change in tilt direction from approximately nearest neighbor in the $L_{c'}$ phase to next nearest neighbor in the $L_{\beta F}$

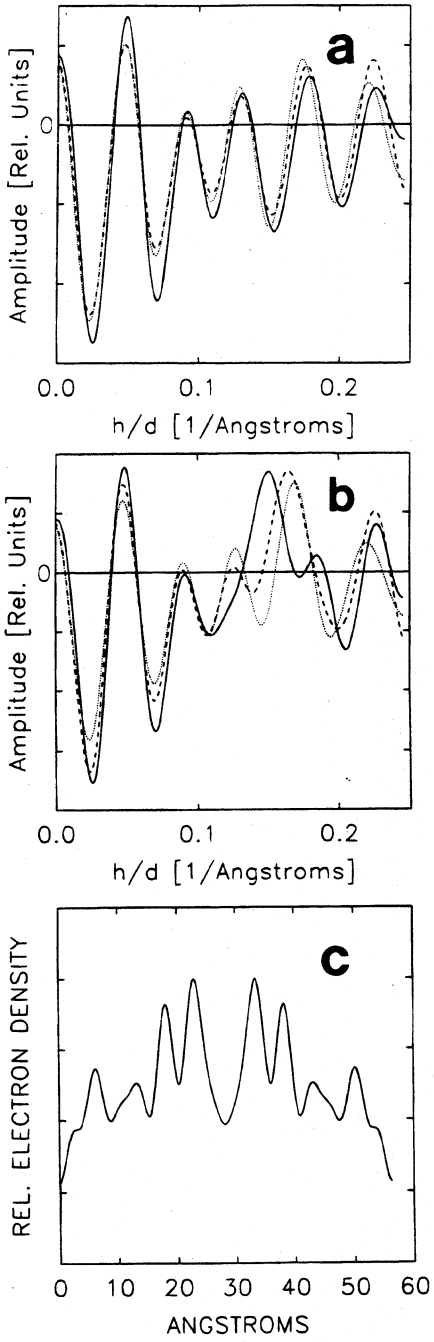

Figure 3. (a) Continuous transforms of $L_{c'}$ DPPC bilayers at RH's of ≈65% (•••), 70% (− − −) and 90% (—) having d spacings of 56.3, 57.1, and 59.0 Å, respectively. (b) Same as (a) except the phase of the ninth order is + instead of −. (c) 1D electron density distribution of 56.3 Å $L_{c'}$ bilayers (65% RH at 17 ± 2 °C) reconstructed to a resolution of ≈4 Å using a phase of + for the ninth-order Bragg reflecton.

phase.[14] In addition, the tilt angle θ decreases by about 10.7°, compared to the $L_{c'}$ phase (Figure 2a), to 26.3°. The two distinct off-equatorial wide-angle reflections (1/4.1 and 1/4.2 Å^{-1}) are the result of the hydrocarbon chains packing in a centered rectangular lattice.[22] Significantly, in addition to the differences in hydrocarbon chain packing between the $L_{c'}$ (Figure 2a) and $L_{\beta F}$ (Figure 2b) phases, the 1D electron density profiles (insets of Figures 2a,b) show that the peaks due to the phosphate moiety of the phosphorylcholine headgroup and the ester groups to be less resolved in the $L_{\beta F}$ phase. This we believe is due to a rapid interconversion, by a change of torsional angles in and

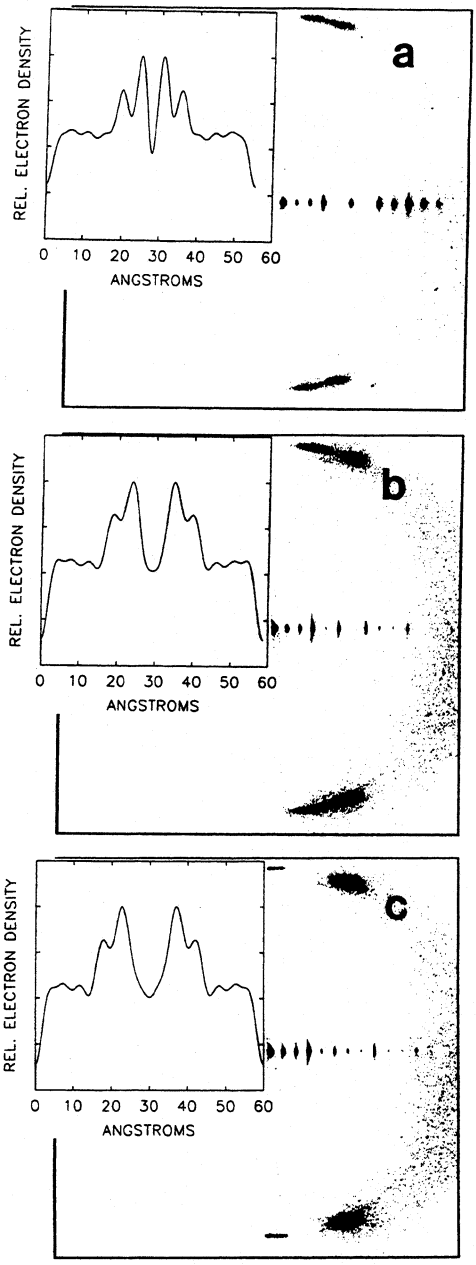

Figure 4. 2D diffraction patterns of $L_{\beta'}$ phase DPPC bilayers at 20 ± 1 °C and various RH's, and their 1D electron density profiles (insets). (a) 0 ± 5% RH bilayers ($L_{\beta F}$ phase) having a d spacing of 55.5 Å, θ of 22.0 ± 0.5°, and a "water region" of 5.7 ± 0.5 Å; (b) 75 ± 10% RH bilayers ($L_{\beta F}$ phase) having a d spacing of 58.6 Å, θ of 28.0 ± 0.5° and a water region of 11.1 ± 0.5 Å; (c) 95 ± 10% RH bilayers ($L_{\beta I}$ phase) having a d spacing of 59.9 Å, a θ of 31.6 ± 0.5°, and a water layer of 14.3 ± 0.5 Å.

near the glycerol backbone, between two (or more) minimum energy conformations in the $L_{\beta F}$ phase.

Figure 4 shows a series of 2D diffraction patterns from oriented DPPC multilayers at 20 °C and various relative humidities along with their 1D electron density profiles (insets). At 0% RH (Figure 4a), the hydrocarbon chains forming a centered rectangular lattice are tilted at an angle θ of ≈22.0° (please see Appendix) toward next nearest neighbors[14] ($L_{\beta F}$ phase, same as in Figure 2b). From the 1D electron density distribution (Figure 4a inset), one can measure the phosphorylcholine headgroups being separated by a "water region" which is ≈5.7 Å thick. In addition, the two most electron-dense peaks due to the ester groups and the phosphate moiety of the phosphorylcholine headgroup are well resolved. At 75% RH (Figure 4b), there is no change in the lattice or the tilt direction, although θ increased by 6.0° to 28.0°. However, at this humidity, the separation between the phosphate groups is ≈11.1 Å, indicating an uptake of water, and the peaks due to the ester groups and phosphate moieties of the phosphorylcholine headgroups are no longer well resolved as was the case in Figure 4a, even though the bilayers have not undergone a phase transition (still in the $L_{\beta F}$ phase as were the 0% RH bilayers). This same effect has also been observed in the 1D electron density profiles constructured by Torbet and Wilkins at various relative humidities.[16]

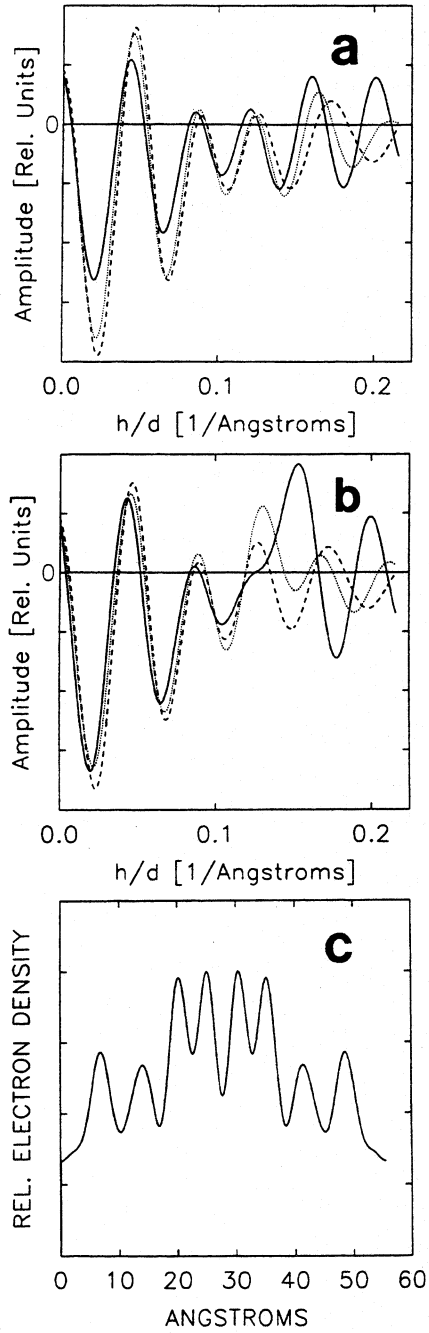

Figure 5. (a) Continuous transforms of various $L_{\beta'}$ DPPC bilayers at RH's of ≈ 0% (– – –), 75% (•••) and 90% (—) having d spacings of 55.5, 58.6, and 59.9 Å, respectively. (b) Same as (a) except the phase of the eighth order is + instead of −. (c) 1D electron density profile of 55.5 Å $L_{\beta'}$ bilayers (0% RH at 20 ± 1 °C) reconstructed to a resolution of ≈4.5 Å using a phase of + for the eighth-order Bragg reflection.

Figure 5 is similar to Figure 3 and justifies the phase choices

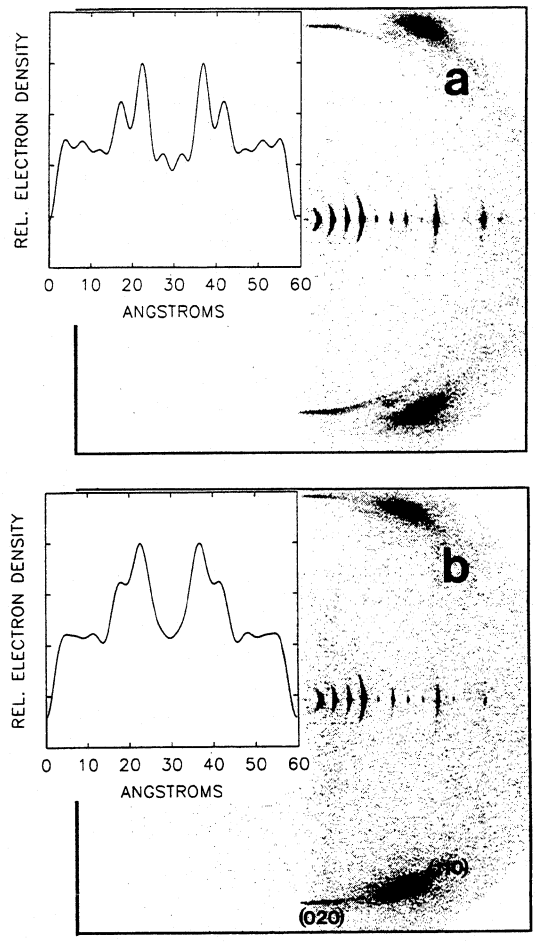

Figure 6. 2D diffraction patterns and 1D electron density profiles (insets) of (a) 85% RH $L_{c'}$ DPPC bilayers having a d spacing of 59.0 Å at 15 ± 2 °C; (b) 59.5 Å $L_{\beta I}$ bilayers at 20 ± 1 °C and 90% RH. The calculated tilt angles θ are 34.7 ± 1.0° and 31.5 ± 0.5° for the $L_{c'}$ and $L_{\beta I}$ phases, respectively. In the $L_{c'}$ phase, the splitting angles measured from the diffraction patterns due to the (020), (1$\bar{1}$0) and (110) reflections are 5.0, 29.3, and 32.3°, respectively. For the $L_{\beta I}$ phase, the splitting angles for the (020) and (110) reflections are 0 and 27.3°, respectively. The (020) and (110) reflections of the $L_{\beta'}$ phase have $1/d$ spacings of 1/4.2 and 1/4.1 Å^{-1}, respectively. The splitting angle measurements contain an error of 0.5° while the d spacings have errors of ±0.3 Å.

used in calculating the different relative humidity electron density profiles found in Figure 4 (insets). However, in this case (Figure 5a) the transforms have expanded much more than those in Figure 3a as a result of θ increasing by ≈10° from 0 to 90% RH. Effectively, increases in θ result in a decrease in the thickness of the bilayer causing the transforms to expand. The transforms presented in Figure 5b were reconstructured using an 8th order structure factor having a phase of + instead of −. The "uniqueness" of the transforms in Figure 5a is destroyed by this simple change (Figure 5b). Finally, Figure 5c shows the electron density distribution of 0% RH bilayers constructed using a phase of + for the eighth-order reflection.

Experiments were also carried out with maximally hydrated DPPC bilayers (d = 59.0 Å at 15 °C) in the $L_{c'}$ phase (Figure 6a), which may better represent the previous excess water studies using powder samples.[3-10] This time the $L_{c'} \rightarrow L_{\beta'}$ phase transition is not accompanied by a change in the molecular tilt direction while the title angle θ experiences a decrease of only 3.2° from 34.7° to 31.5°. In this case, the $L_{\beta I}$ DPPC bilayers[14] (Figure 6b) are practically identical in d spacing (59.5 Å), hydrocarbon chain tilt angle (31.5 ± 0.5°), and molecular tilt direction (toward nearest neighbor) to the DPPC sample presented in Figure 4c.

Discussion

In previous X-ray studies using powder samples to study $L_{c'}$ DPPC bilayers, the (110) and (1$\bar{1}$0) reflections (Figures 2a and 6a) were not differentiated, and as such the hydrocarbon chain lattice was described as being orthorhombic.[4,5,8] Only Cameron and Mantsch,[6] using Fourier transform infrared (FT-IR) spectroscopy, reported results in which the spectra of DPPC bilayers in the $L_{c'}$ phase resembled those found in triclinically packed acyl chains. The triclinic packing motif yields a 2D oblique subcell in the layer.[22]

Glycerol Backbown/Headgroup Differences between Hydrated $L_{c'}$ and $L_{\beta'}$ Bilayers. In the $L_{c'}$ phase (Figures 2a and 6a), we believe that most of the molecular motions near the lipid interface are "frozen out" due to the formation of a 2D molecular lattice.[11] This transition between enantiomeric conformations has been clearly observed in L_α bilayers using ^{31}P and ^{2}H nuclear magnetic resonance (NMR).[23] An FT-IR study on oriented samples of DPPC indicated that the rapid interconversion model was compatible with the experimental data and concluded that the orientation of the ester groups are the same in dry, gel ($L_{\beta'}$), and liquid-crystalline (L_α) bilayers.[24] Recently Dufourc et al.,[25] using ^{31}P NMR line-shape and relaxation measurements, clearly demonstrated free rotation about the P−O (glycerol) bond and hindered rotations about the C_1−C_2 and C_1−O (glycerol) bonds of the glycerol backbone in the $L_{\beta'}$ and L_α phases of dimyristoyl PC (DMPC). It was pointed out that the hindered rotations in and about the glycerol backbone were fast on the NMR timescale even in the $L_{\beta'}$ phase. Of importance, is that in the $L_{\beta'}$ phase the amount of molecular wobble about the bilayer normal was practically nonexistent and the orientation of the headgroup remained unchanged in all of the phases observed in DMPC bilayers.[25] As such, the $L_{c'} \rightarrow L_{\beta F}$ (Figure 2) or $L_{c'} \rightarrow L_{\beta I}$ (Figure 6) phase transitions result in the elimination of the 2D molecular lattice, thus allowing the glycerol backbone to undergo various conformational changes and the phasphorylcholine headgroup to rotate freely. The above-mentioned conformational changes to the glycerol backbone will also cause displacement of the hydrocarbon chains,[23] possibly exposing more of the hydrocarbon chain to the bilayer interface. Cameron and Mantsch[6] noted that the spectrum for the C=O stretching band of $L_{c'}$ DPPC bilayers resembled that of monohydrate and anhydrous DPPC. This was not the case for hydrated bilayers in the $L_{\beta'}$ and L_α phases.[6,26,27]

Changes in the Glycerol Backbone/Headgroup Region as a Function of Hydration. ^{31}P NMR studies as a function of water content and temperature have shown that the addition of water increased the motion of the phosphate group at a fixed temperature in $L_{\beta'}$ bilayers.[28] It was also estimated that only five molecules of water per lipid are necessary to give DPPC the same physical characteristics of fully hydrated molecules.[28,29] Dry $L_{\beta'}$[30] as well as $L_{c'}$ bilayers gave nonaxially symmetric ^{31}P NMR spectra.[3] From the above spectroscopic information, one would expect the 1D electron density profiles of $L_{c'}$ and dry $L_{\beta'}$ bilayers to be similar and to differ from relatively well hydrated $L_{\beta'}$ bilayers. Since the electron density distributions for the different $L_{\beta'}$ phases found in Figures 2b and 4 (insets) were calculated using 11−12 Bragg reflections, we recalculated the $L_{c'}$ profile (Figure 2a) using 11 Bragg reflections, instead of the original 14. This lower resolution electron density profile of $L_{c'}$ bilayers is presented in Figure 7. As one can observe,

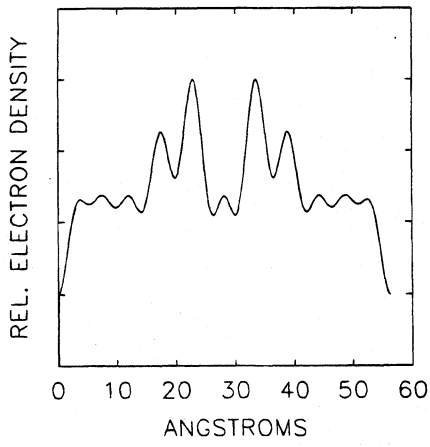

Figure 7. 1D electron density profile of $L_{c'}$ DPPC bilayers found in Figure 2a (inset) and reconstructed using 11 Bragg reflections instead of the 14 used in Figure 2a (inset).

the electron density profile in Figure 7 compares favorably with the dry $L_{\beta'}$ bilayers (Figure 4a), indicating that although water is present in the $L_{c'}$ phase, the motions of the glycerol backbone and the headgroup are restricted due to the presence of a 2D molecular lattice.[11] As such the electron density profiles seem to be in qualitative agreement with the NMR data. Further hydration to the $L_{\beta'}$ bilayers (Figure 4c) does not alter the shapes of the peaks, in the electron density distribution, due to the ester groups and phosphate moiety, consistent with the notion that after some minimum hydration DPPC lipid molecules behave similarly to those which are fully hydrated.[28,29]

Hydrocarbon Chain Tilt Angle θ. With the experiment carried out using maximally hydrated DPPC bilayers in the $L_{c'}$ phase (Figure 6a), it is important to note that the θ's of 56.3 Å (Figure 2a) and 59.0 Å (Figure 6a) $L_{c'}$ bilayers are practically identical, while those of $L_{\beta'}$ bilayers change significantly as a function of hydration (Figure 4) up to a limiting value of 32 ± 1°.[13,31] It should be pointed out that this limiting value of θ is achieved at less than excess water conditions[12] as shown in Figure 4c, in which 100% RH bilayers have a d spacing of only 59.9 Å and a θ of 31.6°. Levine concluded that there was no change in θ from ≈7.2 waters/lipid to full hydration at ≈10.2 waters/lipid.[32] In a recent study, it was determined that at full hydration $L_{\beta'}$ DPPC bilayers contain ≈11.8 waters/lipid.[13] It therefore seems that the formation of a molecular lattice[11] in the $L_{c'}$ phase restricts the further binding of water molecules to the headgroup region of the lipid and as such, θ in the $L_{c'}$ phase may be practically independent of the water molecules present in the system, unlike $L_{\beta'}$ bilayers, whose continual binding of water, up to a certain maximum, affects the hydrocarbon chain tilt angle. However, we should stress that further experiments in the low hydration regime of the $L_{c'}$ phase should be carried out to verify this result.

Recently it was demonstrated, using PC's whose chain length was increased from 16 to 20 carbons, that θ increased by 3° if the area/hydrocarbon chain, measured perpendicular to the long axis of the chains, decreased by 0.5 Å^2.[13] If this is the case in the $L_{c'}$ phase, the greater value of θ in the $L_{c'}$ phase compared to the $L_{\beta'}$ phase can be accounted for by the fact that the area/hydrocarbon chain is ≈3% less in $L_{c'}$ bilayers (Figure 6a) (19.1 ± 0.2 vs 19.7 ± 0.1 Å^2) compared to $L_{\beta'}$ bilayers (Figure 6b).

Concluding Remarks

We have found that the $L_{c'} \rightarrow L_{\beta'}$ phase transition involves a change in hydrocarbon chain packing (oblique centered to centered rectangular), tilt angle, and direction, depending on the initial hydration of the $L_{c'}$ bilayers. In addition it was shown that the electron density profiles of $L_{c'}$ bilayers resembled those of dry $L_{\beta'}$ bilayers in the bilayer interface region, consistent with NMR data. We believe that the presence of a 2D molecular lattice in the $L_{c'}$ phase inhibits the various conformational changes that are normally undertaken in hydrated $L_{\beta'}$ bilayers. Removal of practically all the water has the same effect as was shown by the 1D electron density profile of dry DPPC bilayers. The hydrated $L_{\beta'}$ bilayers (both $L_{\beta F}$ and $L_{\beta I}$ phases) differ from the $L_{c'}$ and dry $L_{\beta'}$ bilayers in that they exhibit a greater mobility at the bilayer interface, possibly resulting in the greater hydration of the C=O groups. Finally, it seems that the chain tilt angle and direction in $L_{c'}$ bilayers may be unaffected by changes in hydration, unlike $L_{\beta'}$ bilayers.

Appendix

The calculation of the chain tilt angle θ, with respect to the bilayer normal, from the measured splitting angles depends on the direction of the molecular tilt in a given lattice. For example, if the molecules are tilted between nearest neighbors ($\phi = 0°$) (Figures 2b and 4a,b), then the azimuthal angle ϕ is related to the tilt angle θ by the following expression:

$$\sin \psi_{200} = \pm \cos 0° \sin \theta^{32}$$

It is therefore clear that to a first approximation the splitting angle ψ is equal to the tilt angle θ.

In the situation where we have an oblique lattice with a molecular tilt toward ($\phi = 30°$) or very close to nearest neighbors (e.g., Figures 2a and 6a), the problem is slightly more complicated. First we must introduce the concept of lattice spacings. In Figure 2a the diffraction pattern contains three distinct wide-angle reflections labeled (020), (110), and ($1\bar{1}0$). The (020) reflection is practically centered on the equatorial axis (perpendicular to c^*) and thus has a repeat spacing (d) equal to its lattice spacing. However, the lattice spacings of the (110) and ($1\bar{1}0$) reflections are given by their projections on to the equatorial axis (axis perpendicular to the c^* axis). In the following formula, the projections for the various reflections are labeled d'. The tilt angle θ is therefore obtained in the following manner:

$$\frac{a^2}{b^2} = \left[2\left(\frac{d'_{020}}{d'_{1\bar{1}0}}\right)^2 + 2\left(\frac{d'_{020}}{d'_{110}}\right)^2\right] - 1$$

where a and b are the 2D unit-cell dimensions. Since a and b are both unknown, we need to independently solve for one of the two. a can thus be obtained using

$$a = \sqrt{4(d'_{020})^2 / \left\{1 - \frac{b^2}{a^2}\left[\left(\frac{d'_{020}}{d'_{1\bar{1}0}}\right)^2 - \left(\frac{d'_{020}}{d'_{110}}\right)^2\right]^2\right\}}$$

b can then easily be solved from the previous expression of a^2/b^2. The hydrocarbon chain tilt angle θ is then given by

$$\theta = [\tan^{-1}(\tan \psi_{1\bar{1}0}/\sin \omega_{1\bar{1}0}) + \tan^{-1}(\tan \psi_{110}/\sin \omega_{110})]/2$$

where, for example, $\sin \omega_{110}$ equals d'_{110}/b and ψ_{110} is the splitting angle of the (110). The same calculations can be used to obtain the lattice parameters a and b, and the tilt angle θ for an orthorhombic nearest-neighbor molecular tilt ($\phi = 30°$) system (Figure 4c and 6b) except that now $d'_{110} = d'_{1\bar{1}0}$.

Acknowledgment. Many stimulating discussions with V. A. Raghunathan and S. Tristram-Nagle along with technical

assistance from P. Meleard, R. Bernon, G. Raffard, and C. Grant are gratefully acknowledged. The author would also like to thank the Natural Sciences and Engineering Research Council of Canada for a fellowship and the Centre de Recherche Paul Pascal, through the many efforts of Drs. Jean Dufourcq and Erick J. Dufourc on the author's behalf, for further financial support.

References and Notes

(1) Abbreviations: DPPC, 1,2-dipalmitoyl-*sn*-glycero-3-phosphatidylcholine; $L_{c'}$ phase, subgel phase; $L_{\beta'}$ phase, gel phase; θ, hydrocarbon chain tilt angle.

(2) Chen, S. C.; Sturtevant, J. M.; Gaffney, B. J. *Proc. Natl. Acad. Sci. U.S.A.* **1980**, *77*, 5060.

(3) Füldner, H. H. *Biochemistry* **1981**, *20*, 5707.

(4) Ruocco, M. J.; Shipley, G. G. *Biochim. Biophys. Acta* **1982**, *684*, 59.

(5) Ruocco, M. J.; Shipley, G. G. *Biochim. Biophys. Acta* **1982**, *691*, 309.

(6) Cameron, D. G.; Mantsch, H. H. *Biophys. J.* **1982**, *38*, 175.

(7) Stümpel, J.; Eibl, H.; Nicksch, A. *Biochim. Biophys. Acta* **1983**, *727*, 246.

(8) Church, S. E.; Griffiths, D. J.; Lewis, R. N. A. H.; McElhaney, R. N.; Wickman, H. H. *Biophys. J.* **1986**, *49*, 597.

(9) McIntosh, T. J.; Simon, S. A. *Biochemistry* **1993**, *32*, 8374.

(10) Tristram-Nagle, S.; Suter, R. M.; Sun, W.-J.; Nagle, J. F. *Biochim. Biophys. Acta* **1994**, *1191*, 14.

(11) Katsaras, J.; Raghunathan, V. A.; Dufourc, E. J.; Dufourcq, J. *Biochemistry*, accepted.

(12) Excess water preparations (e.g., 50:50 lipid−water ratio by weight) are not equivalent to 100% RH samples. Excess water samples of DPPC have d spacings of ≈64 Å while 100% RH DPPC samples generally have d spacings approaching 60 Å. However, it is important to note that the hydrocarbon chain tilt direction and tilt angle θ are the same for both.

(13) Tristram-Nagle, S.; Zhang, R.; Suter, R. M.; Worthington, C. R.; Sun, W.-J.; Nagle, J. F. *Biophys. J.* **1993**, *64*, 1097.

(14) Smith, G. S.; Sirota, E. B.; Safinya, C. R.; Clark, N. A. *Phys. Rev. Lett.* **1988**, *60*, 813. The $L_{\beta'}$ phase is in fact three distinct 2D phases which are distinguishable by their hydrocarbon chain tilt direction. In the low-RH $L_{\beta F}$ and high-RH $L_{\beta I}$ phases the hydrcarbon chains are tilted between nearest neighbors and toward nearest neighbors, respectively. The $L_{\beta L}$ phase is an intermediate phase not found in thermotropic systems: Leadbetter, A. P.; Gaughan, J. P.; Kelly, B.; Gray, G. W.; Goodby, J. *J. Phys.* **1979**, *C3 40*, 178.

(15) Worthington, C. R.; McIntosh, T. J. *Nat. New Biol.* **1973**, *245*, 97.

(16) Torbet, J.; Wilkins, M. H. F. *J. Theor. Biol.* **1976**, *62*, 447.

(17) Katsaras, J.; Jeffrey, K. R.; Yang, D. S. C.; Epand, R. M. *Biochemistry* **1993**, *32*, 10700.

(18) Shannon, C. E. *Proc. Inst. Radio Engrs., N.Y.* **1949**, *37*, 10.

(19) Sayre, D. *Acta. Crystallogr.* **1952**, *B5*, 843.

(20) Franks, N. P. *J. Mol. Biol.* **1976**, *100*, 345.

(21) Katasaras, J.; Stinson, R. H.; Davis, J. H.; Kendall, E. J. *Biophys. J.* **1991**, *59*, 645.

(22) Jacquemain, D.; Leveiller, F.; Weinbach, S. P.; Lahav, M.; Leiserowitz, L.; Kjaer, K.; Als-Nielsen, J. *J. Am. Chem. Soc.* **1991**, *113*, 7684. Kenn, R. M.; Böhm, C.; Bibo, A. M.; Peterson, I. R.; Möhwald, H.; Als-Nielsen, J.; Kjaer, K. *J. Phys. Chem.* **1991**, *95*, 2092.

(23) Hauser, H.; Pascher, I.; Sundell, S. *Biochemistry* **1990**, *27*, 9166. Seelig, J.; Gally, H. U.; Wohlgemuth, R. *Biochim. Biophys. Acta* **1977**, *467*, 109.

(24) Hübner, W.; Mantsch, H. H. *Biophys. J.* **1991**, *59*, 1261.

(25) Dufourc, E. J.; Mayer, C.; Stohrer, J.; Althoff, G.; Kothe, G. *Biophys. J.* **1992**, *61*, 42.

(26) Lewis, R. N. A. H.; McElhaney, R. N. *Biochemistry* **1990**, *29*, 7946.

(27) Blume, A.; Hübner, W.; Messner, G. *Biochemistry* **1988**, *27*, 8239.

(28) Arnold, K.; Löbel, E.; Volke, F.; Gawrisch, K. *Stud. Biophys.* **1981**, *3*, 207.

(29) Volke, F.; Arnold, K.; Gawrisch, K. *Chem. Phys. Lipids* **1982**, *31*, 179.

(30) Katsaras, J.; Yang, D. S.-C.; Epand, R. M. *Biophys. J.* **1992**, *63*, 1170. $L_{\beta F}$ bilayers exist over a broad range of RH's.

(31) Tardieu, A.; Luzzati, V.; Reman, F. C. *J. Mol. Biol.* **1973**, *75*, 711.

(32) Levine, Y. K. *Prog. Biophys. Mol. Biol.* **1972**, *24*, 3. Levine, Y. K. *Prog. Surf. Sci.* **1973**, *3*, 279.

JP941604Q